Journal of Rock Mechanics and Geotechnical Engineering 13 (2021) 46–59

Contents lists available at ScienceDirect

Journal of Rock Mechanics and Geotechnical Engineering

journal homepage: www.jrmge.cn

Nominated Qian Lecture

Principles and methods of rock support for rockburst control

Charlie Chunlin Li

Norwegian University of Science and Technology (NTNU), Trondheim, Norway

ARTICLE INFO

Article history:
Received 12 October 2020
Received in revised form
6 November 2020
Accepted 11 November 2020
Available online 3 December 2020

Keywords:
Rock support
Rockburst
Rockbolt
Yield rockbolt
Mesh
Shotcrete

ABSTRACT

This paper presents the principles of rock support for rockburst control and three rockburst support systems used in deep metal mines. Before the principles of rock support are presented, rock fracture related to strain burst is first discussed with the help of photos taken on site, and the energy sources and transformations during bursting are illustrated through conceptual models. Surface parallel extension fracture usually occurs in the ejected and surrounding rocks in a strain burst event, while the ejected rock in a fault-slip rockburst is often already pre-fractured before the event. There must be excessive release energy available for rock ejection. The excessive release energy comes from both the ejected rock itself and the surrounding rock. To prevent rock ejection in a rockburst, the support system must be able to dissipate the excessive release energy. All support devices in a support system for rockburst control must be able to dissipate energy, be firmly linked, and be compatible in deformability. A support system for rockburst control comprises surface-retaining devices and yield rockbolts as well as yield cablebolts when needed. Laying mesh on the top of shotcrete liner is a good practice to enhance the surface-retaining capacity of the support system. Energy-absorbing yield rockbolts dissipate energy either by stretching of the bolt shank or by sliding of the inner anchor in the borehole. Mesh, mesh strap and shotcrete are the surface-retaining devices widely used in the current rock support systems. The three types of rock support used for rockburst control at present are soft support system using Split Set bolts, hybrid support system using rebar and two-point anchored yield bolts, and entirely yieldable support system using strong yield bolts.

1. Introduction

Rockburst is a major instability issue in underground excavation. Tremendous efforts have been made to understand the mechanisms of rockburst in order to control it by appropriate rock support systems in the past decades (e.g. Morrison, 1942; Duvall and Stephenson, 1965; Salamon, 1983; Morrison et al., 1996; Ortlepp, 1997; He et al., 2010; Shan and Yan, 2010; Feng et al., 2012, 2018; Li et al., 2017; Su et al., 2017; Tarasov and Stacey, 2017; Kaiser, 2018). In a rockburst, rock is ejected or remarkably displaced. It is logical to think to use ductile support devices to control the rock displacement. Therefore, Split Set friction bolts were first used to combat rockburst threats in South African mines in the 1950s and 1960s. A Split Set bolt is held in the borehole by the friction between the bolt tube and the borehole wall. It cannot efficiently restrain the rock displacement because of its low load-bearing capacity. People also attempted to use stiff support devices, such as fully encapsulated rebar bolts and concrete pillars, to deal with dynamic loads. The results, however, were not convincing. It was observed in mines that some fully grouted rebar bolts brittlely ruptured after the rockburst events, such as those snapped rebar bolts shown in Fig. 1a. The concrete pillars set up in the mine drifts were seriously damaged or blown up after a large blast in a mine stope nearby in a Canadian deep mine (Fig. 1b). Having recognized the limitations of both ductile and stiff support devices in rockburst control, Cook and Ortlepp (1968) proposed the concept of yield support. They demonstrated the power of yield rockbolts in reducing the rock damage in a mine drift through a blast trial in a mine drift (Ortlepp, 1969; Stacey 2012).

In the 1990s, the first yield rockbolt for rockburst control, that is, the cone bolt, was developed in South Africa (Jager, 1992; Ortlepp, 1992). The original version of the cone bolt was fully encapsulated in the borehole with cementitious grout. It was modified later for use with resin grout in Canada (e.g. Simser, 2001; Simser et al., 2006). After that, several other types of energy-absorbing yield rockbolts were invented (e.g. Varden et al., 2008; Li, 2010; Wu and

E-mail address: charlie.c.li@ntnu.no.

Peer review under responsibility of Institute of Rock and Soil Mechanics, Chinese Academy of Sciences.

https://doi.org/10.1016/j.jrmge.2020.11.001

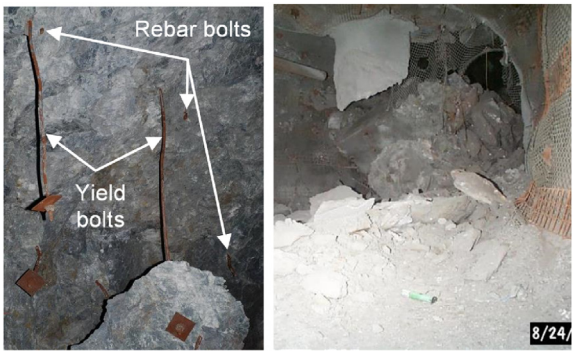

Fig. 1. Consequences of stiff support devices under strong dynamics loading: (a) Ruptured fully encapsulated rebar bolts in a rockburst (Li, 2019), and (b) the blow-up failure of a stiff concrete pillar after an operation blast in a mine (photo by B. Simser).

Oldsen, 2010; He et al., 2014; Darlington et al., 2018; Knox and Berghorst, 2019). Along with yield rockbolts, surface-retaining devices are also obligatory for satisfactory rockburst control. It is required that both the internal and external support devices in a support system must be firmly linked and be compatible in deformability in order that all the devices are properly interacted and together provide resistance to the rock ejection in a rockburst.

The purpose of this paper is not to provide a review over all support methods that have been tried or used in the rock support practice. Instead, it aims to present new thoughts on the principles of rock support for rockburst control, based on the author's own rock support practice, field observations and academic studies but also with references to work by others. In the paper, field observations of rock fracture patterns related to rockburst are first presented. The energy sources and energy transformations in a rockburst event are explained with the help of two conceptual models. The principles of rock support for rockburst control are then derived from the point of view of energy release and dissipation. Finally, a support methodology is proposed. The requirements for support devices and the factor of safety are discussed. Full-scale impact tests of two support arrangements are briefly presented to demonstrate the proportions of energy dissipated in the reinforcing rockbolts and the surface-retaining mesh. Finally, three support systems for rockburst control used in three countries are introduced. The three support systems are developed based on different philosophies.

2. Rock failure in burst-prone rock mass

2.1. Rock failure in hard rock

2.1.1. Fracture patterns

It is often observed in the field that fractures are tightly spaced both in the ejected rock and in the surrounding rock after the occurrence of a strain burst in massive hard rock. The fractures are parallel with the excavation surfaces, and the spacing between the fractures varies from millimeters to decimeters. The fracture zone could extend for several meters in the surrounding rock.

Fig. 2 shows the fractures exposed on the excavation face of a mine stope in a deep gold mine in South Africa. The ore rock was extremely hard and brittle quartzite with the uniaxial compressive strength (UCS) up to 300–400 MPa. The mine stope was at a depth of approximately 3000 m. The vertical in situ stress was approximately 80 MPa. The stope was 1–1.5 m high, and the excavation

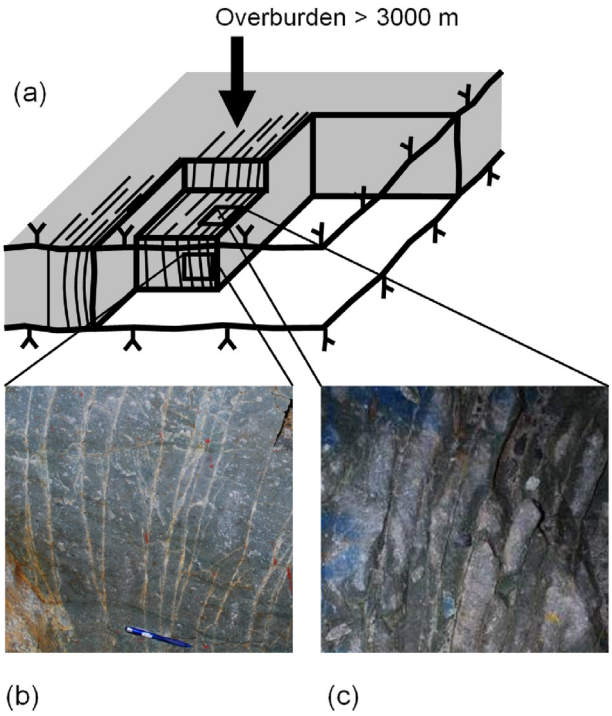

Fig. 2. Surface-parallel fractures created by high vertical stress in the hard rock ahead of the advance face of a mine stope in a deep gold mine in South Africa. (a) A perspective view of the mine stope, (b) the fractures exposed on a vertical cut perpendicular to the advance face, and (c) the fractures exposed on a horizontal bench (Li, 2017a).

face was advanced by 1–1.5 m after every blast round. The surface-parallel fractures extended for meters in the rock ahead of the face. Strain burst frequently occurred on the face and the rock slabs were ejected into the stope void.

Fig. 3 shows another example of stress-induced fractures exposed on the excavation face of a crosscut toward the second slice (Cut 2) of a cut-and-fill mine stope at a depth of 1000 m in a massive hard quartzite rock mass. Only a few pre-existing geological discontinuities had been exposed on the excavation face but intensive strain burst occurred on the roof in the bottom slice (Cut 1) of the stope. The surface burst was accompanied by frequent brittle snapping noises. The surface burst disappeared after a few hours, but powerful bursting sounds intermittently emitted from the depths of the surrounding rock. The powerful sounds were associated with rock fracturing inside the surrounding rock, including the rock in the roof. The sub-horizontal fractures shown in the figure were created during the excavation of Cut 1. The thickness of the rock slabs between the fractures varied from 3 cm to 10 cm.

Surface-parallel fractures are created in overstressed areas where the tangential stress is relatively uniformly distributed, as shown in Figs. 2 and 3. In areas where the stress gradient is large, such as in the bottom of a strain burst pit, the fractures are spaced tightly in the center of the stress concentration and radiate outward, as shown in Fig. 4.

Surface-parallel fracture in the rock is formed under the compressive tangential stress, but its nature is of extension. The term of extension fracture is used in this paper to distinguish tensile fracture under tensile stress. Martin and Chandler (1994) defined crack initiation stress σ_{ci} and crack damage stress σ_{cd} on the uniaxial compressive stress–strain curve of rock. It is said that the crack initiation stress is 40%–60% of the peak strength σ_p which is the UCS of the rock in the laboratory, and the crack damage stress

Fig. 3. Stress-induced horizontal rock slabs in the roof of a cut-and-fill mine stope at a depth of 1000 m (Li, 2019).

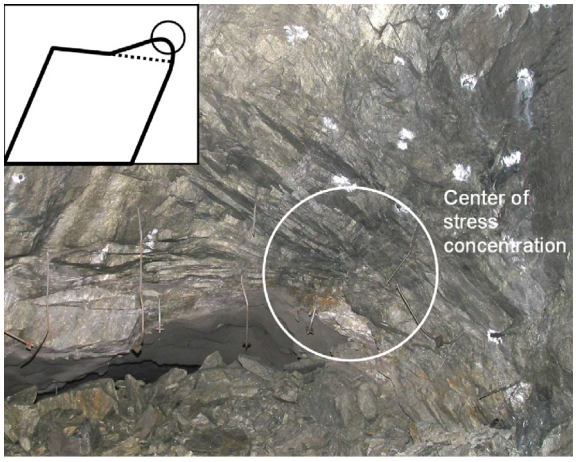

Fig. 4. The stress concentration center in the bottom of the strain burst pit in a cut-and-fill mine stope and the radially oriented extension fractures exposed on the excavation face of a subsequent slice cut in the stope (Li, 2017a).

is 70%–90% of σ_p. It is claimed that cracks grow stably in the range from σ_{ci} to σ_{cd} while the crack propagation becomes unstable when the stress is above σ_{cd}. Li and Nordlund (1993) carried out uniaxial compression tests on Kuru granite samples. The samples were loaded under different loading conditions: monotonic loading, cyclic loading with a delay time between loading cycles, and cyclic loading with a holding time at the ultimate load of every cycle. The UCS, or the short-term peak strength, of the granite sample under the monotonic loading was 260 MPa. The UCS of all other samples tested under cyclic loading was lower, ranging from 215 MPa to 251 MPa. Obviously, the cyclic loading caused damages to the samples so that the UCS became reduced. That is in agreement with the statement by Martin and Chandler (1994) that accumulated damages in the rock could result in reduction in the strength. A Kuru granite sample was tested by holding the load at 64 MPa, 114 MPa, 167 MPa and 215 MPa, which correspond to 25%, 44%, 64% and 82% of the peak strength (260 MPa) of the rock, respectively. Fig. 5 shows the acoustic emissions (AEs) registered during the holding time (1 h) under the four load levels. AEs above the threshold (48 dB) disappeared immediately when the loading stopped and the load was held at 25% of σ_p (Fig. 5a). Holding at the level of 44% of σ_p, the AE continued but became attenuated to a remarkably low level after approximately 2000 s (Fig. 5b). Holding at the level of 64% of σ_p, the AE continued and remained active during the holding time (Fig. 5c). Holding at the level of 82% of σ_p, the AE accelerated with time and finally failed after approximately 300 s since holding started (Fig. 5d). The AE monitoring results in Fig. 5 indicate that:

(1) Extension crack growth indeed occurs in load levels between σ_{ci} and σ_{cd};
(2) Macroscopic extension fracture could occur when the load is 40%–50% of σ_p under long-term loading so that the postulate that the long-term strength of rock is approximately 50% of σ_p is reasonable;
(3) Fracturing accelerates when the load is at a level higher than 80% of σ_p, which supported the statement by Martin and Chandler (1994). The field tests carried out by Andersson et al. (2009) also supported that the extension strength of rock is approximately 50% of σ_p.

Based on limited field observations and philosophical thinking, Diederichs (2003) proposed a conceptual criterion for extension fracture. He distinguished the strengths of brittle and hard rocks under short- and long-term loading conditions and presented the short- and long-term strengths in a diagram, as shown in Fig. 6. The upper thicker curve represents the short-term strength of rock samples in the laboratory. The failure mode of the rock is mixed with extension and shear fractures under low confining stress and is pure shear failure under high confining stress. The lower thinner curve in the diagram represents the long-term strength of rock in situ, the failure mode of which is of extension. The surrounding rock is under long-term loading conditions in an excavation-completed tunnel or in the region more than 2 times the tunnel diameter behind the excavation face in a tunnel under excavation (Fig. 7a). The spalling strength of the rock in that region is described by the thinner curve in the diagram. In the region immediately behind the excavation face, from the face to a distance of approximately 2 times the tunnel diameter, the load-rising time in the surrounding rock is several hours or days depending on the excavation speed. The loading condition in that region belongs neither to short term as in laboratory tests nor to long term as in the region far behind the face. It is essentially under a medium-term loading condition. The rock in the region immediately behind the face could be subjected to extension fracture (spalling) and even strain burst when the load levels are higher than the long-term strength (Fig. 7b). The hatched area between the long- and short-term strength curves in Fig. 6 possibly describes the medium-term strength of the rock.

2.1.2. Strain burst

When overstressed hard rock fails, the strain energy stored in the rock is released abruptly to eject rock. This is called strain burst. Strain burst is often self-initiated when the tangential stress in the surrounding rock is great enough after excavation, but it could be also triggered by a seismic disturbance when the tangential stress is slightly smaller than the failure limit. In these cases, the intensity of a strain burst is mainly associated with the strain energy released from the rock. Fig. 8a shows a self-initiated strain burst that occurred at a depth of approximately 1000 m in a massive quartzite rock mass. The rock debris in the burst pile is typically thin plates with knife-sharp edges. In other cases, seismic waves could both trigger a strain burst and contribute energy for rock fragmentation. Fig. 8b shows a strain burst that might be triggered by a strong fault-slip seismicity event. The rock was heavily fragmented to small cubic pieces during the burst. It was believed that the rock was intact before the event and the fine fragmentation might be due to a significant amount of energy input from the fault-slip seismicity in addition to the strain energy released from the rock mass.

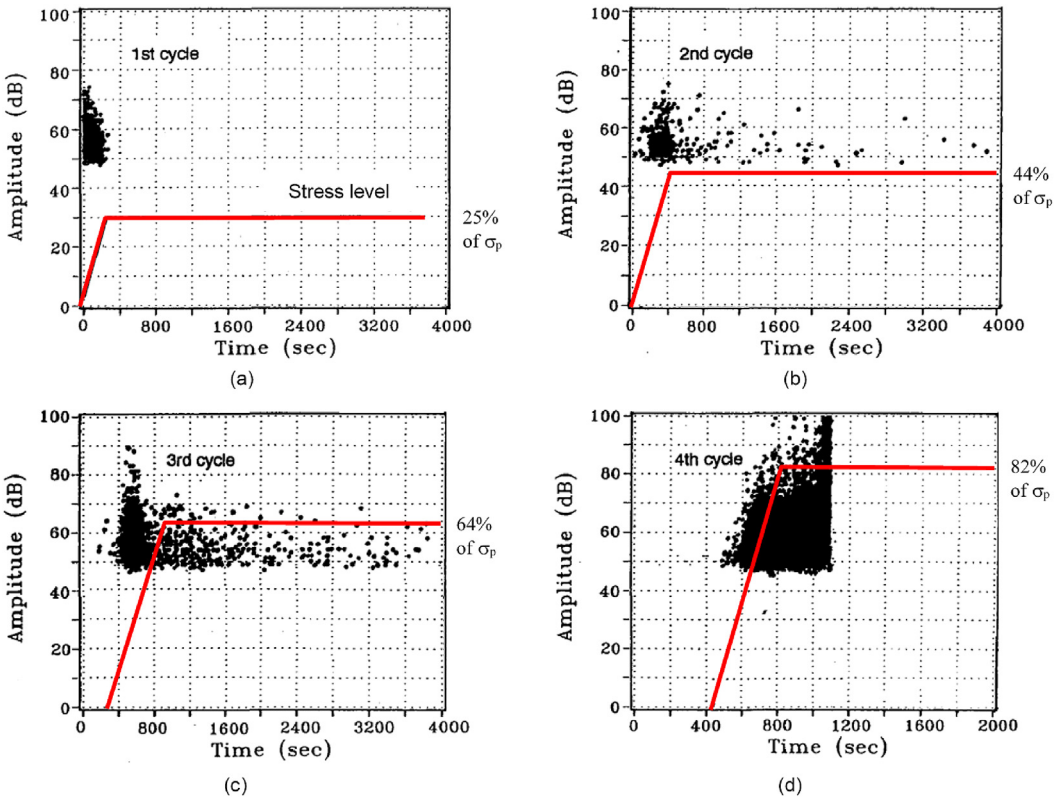

Fig. 5. Acoustic emissions registered on a Kuru granite sample (FIN14) versus time at four holding load levels: (a) 25%, (b) 44%, (c) 64% and (d) 82% of σ_p. The dots represent the magnitudes of the acoustic emission events and the red lines are the loading paths. The holding time was 1 h at the first three load levels. The percentage of the holding load levels is with respect to the short-term UCS (260 MPa) of the rock that was measured on another rock sample. Modified from Li and Nordlund (1993).

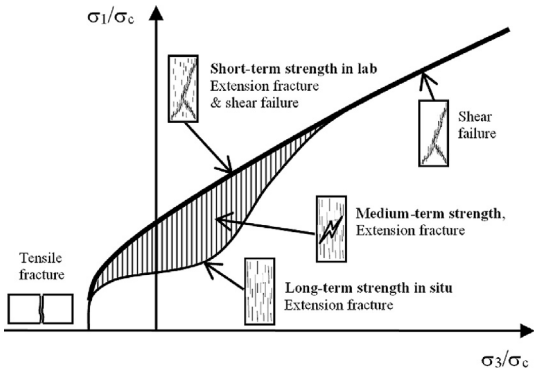

Fig. 6. Schematic diagram showing the short-, medium- and long-term strengths of rocks and corresponding failure mechanisms. σ_c is the short-term UCS of rock sample. Modified from the diagram by Diederichs (2003).

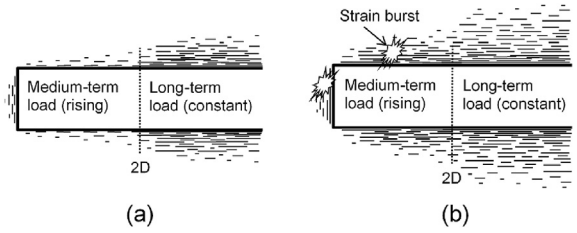

Fig. 7. Sketches illustrating the rock fracture patterns in regions under long- and medium-term loading conditions in hard rock masses of (a) moderate in situ stresses and (b) high in situ stresses.

2.2. Rock failure in moderately hard rock

Underground excavation changes the stress state in the surrounding rock. Pre-existing faults nearby may be mobilized so that slippage occurs along the faults. A mine seismicity event is thus generated. In an overstressed moderately strong rock mass, the surrounding rock could be already failed under the concentration of static stresses. When the seismic waves reach the underground opening, the pre-failed wall rock may be ejected, thus triggering a fault-slip rockburst (Fig. 9). Fault slippage usually releases a significant amount of energy. Therefore, a fault-slip rockburst may cause more serious damages to underground infrastructures than a strain burst does. Rock debris from a fault-slip rockburst comprises rock pieces of various sizes, ranging from finely fragmented debris to large blocks. Fig. 10 shows the rock pile after a fault-slip rockburst in a deep metal mine. That burst was triggered by a fault-slip in the rock mass about 100 m far from the burst place. A rockburst triggered by a fault-slip may be more powerful than a strain burst because of the considerable amount of energy input from the seismic waves.

3. Energy transformations in a rockburst event

3.1. Energy sources and dissipations

A self-initiated strain burst in hard rock is directly caused by the elevated tangential stress in the surrounding rock after excavation. The stress state in the rock is typically elastic prior to rock ejection. The sources of the released energy and the targets for dissipation of the energy can be illustrated with the help of the ball-cliff conceptual model presented in Fig. 11. That model was further

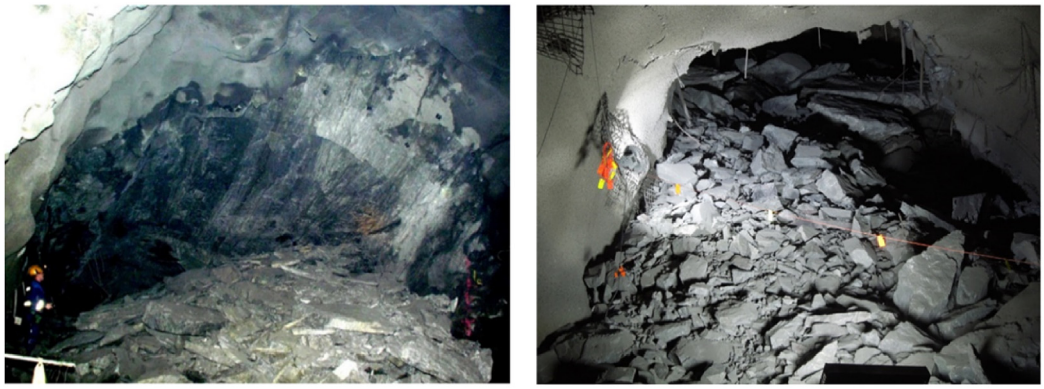

(a) (b)

Fig. 8. (a) A self-initiated strain burst at a depth of 1000 m in a hard quartzite orebody, and (b) a strain burst triggered by a fault-slip seismicity event at a depth of 1100 m in a deep metal mine.

developed based on a model proposed by Li (2019). In the conceptual model, the ball stands for the ejected rock and the cliff edge for the rock strength. The ball is on the left side to the cliff if the tangential stress is less than the rock strength. The ball is on the right side if the rock fails and bursts. The distance from the ball to the cliff edge on the left stands for how far the tangential stress is to the level of the rock strength. The released strain energy increases with both the stress state and the volume of the ejected rock, which is represented by the cliff height, W_e, in Fig. 11. In addition, a certain amount of seismic wave energy is transferred to the ejected rock when the burst is triggered by a seismic event. The seismic energy is represented by W_s in the model. The closer the ball on the left side is to the cliff, the more likely the burst will occur. The total released energy, that is, the sum of the strain energy W_e and the seismic energy W_s, is dissipated for rock fracture (W_f), vibration and heat (W_v), and rock ejection (W_k). Whether a burst occurs and how powerful it is dependent on how much the kinetic energy W_k is.

The model is valid for both strainburst and fault-slip rockburst. Fig. 12a shows the conceptual model for self-initiated strain burst. In a self-initiated strain burst, the released strain energy W_e is the sole energy source. The prerequisites for strain burst are that the tangential stress in the rock must reach the level of the rock strength, and there must be excessive energy for rock ejection, i.e. $W_k > 0$. Fig. 12b presents the model for fault-slip rockburst. The rock subjected to fault-slip rockburst is often pre-fractured prior to the burst event so that the kinetic energy for rockburst may be primarily provided by seismic waves in a fault-slip rockburst. In other words, the seismic energy input W_s is usually much larger than the strain energy W_e.

3.2. Energy transformations during bursting

There are two types of post-peak behavior in rock (Wawersik and Fairhurst, 1970). Class I rock needs external energy input for further deformation in the post-peak stage, but Class II rock releases a portion of its excessive energy after failure. Fig. 13 shows the stress–strain curves of two rock samples of the two classes. Strain burst often occurs in Class II rock, but fault-slip rockburst occurs in both Class I and Class II rocks.

The energy transformations during a rockburst are illustrated in Fig. 14. The thinner solid curve to the left describes the load–displacement behavior of the rock. The peak load at *A* represents the rock strength. The strain energy stored in the rock prior to failure is represented by the area bounded by *OABO*. Some of the energy, W_{bf}, is dissipated by rock fracture in the post-peak stage, and the remaining portion, W_{bk}, is transformed into kinetic energy to eject rock neglecting the part for vibration and heat. The thicker solid line to the right (*AC*) is the response line of the surrounding rock during rock failure. The slope of the line represents the overall stiffness of the surrounding rock in the position of the rock failure on site. The elastic strain energy released from the surrounding rock is represented by the triangle bounded by *ACBA*. A portion of this energy, W_{mf}, is dissipated by rock fracture, and the other portion, W_{mk}, is transformed into kinetic energy. The total released strain energy W_e is the total areas bounded by *OACBO*, i.e. $W_e = (W_{bf} + W_{bk}) + (W_{mf} + W_{mk})$. In addition to the released strain energy, there is an extra energy input W_s from the seismic waves in fault-slip rockburst. The total released energy W is the sum of the released strain energy and the seismic energy input, i.e. $W = W_e + W_s$. The energy dissipated for rock fracture, W_f, is the sum of W_{bf}, W_{mf} and W_{sf}, i.e. $W_f = W_{bf} + W_{mf} + W_{sf}$, where W_{sf} is the rock fracture energy contributed by the seismicity. The kinetic energy for rock ejection, W_k, is the sum of W_{bk}, W_{mk} and W_{sk}, i.e. $W_k = W_{bk} + W_{mk} + W_{sk}$, where W_{sk} is the kinetic energy contributed by the seismicity. In other words, the kinetic energy of the ejected rock comes from the rock itself, the surrounding rock mass, and the seismic waves. The kinetic energy contributed by the ejected rock itself, W_{bk}, depends on the rock type, and it is a constant per unit volume for a given rock type. However, the kinetic energy coming from the surrounding rock, W_{mk}, is associated with the displacement, therefore the stiffness, of the rock mass.

4. Principles and requirements of rockburst support

4.1. Principles

In a rock mass with rock reinforcement, the total amount of released energy of the rock mass is dissipated by rock fracture and the rock support system as well by rock ejection in the case that the rock support system fails. To eliminate rock ejection, it is required that the energy absorption of the support system, W_{rs}, must be larger than the remaining released energy after rock fracture, i.e.

$$W_{rs} > W - W_f \tag{1}$$

For a given amount of released energy, *W*, the more the energy dissipated by rock fracture is, the less energy the support system needs to dissipate. It has been found that support systems with strong surface-retaining devices are favorable in enhancing the energy dissipation by rock fracture. Fig. 15 shows such a support system comprising chain link meshes, mesh straps, and energy-

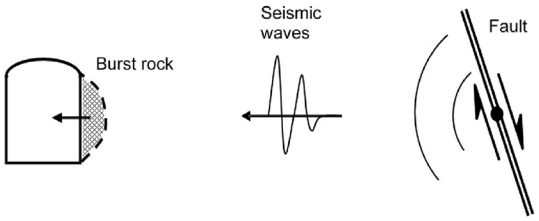

Fig. 9. Schematic for fault-slip rockburst caused by fault slippage (Li, 2017a).

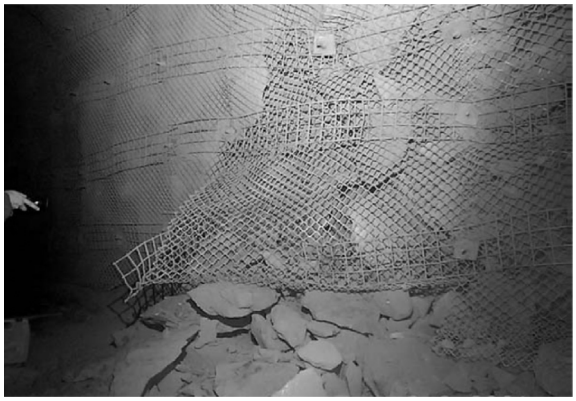

Fig. 10. A fault-slip rockburst in a deep metal mine (Simser, 2001).

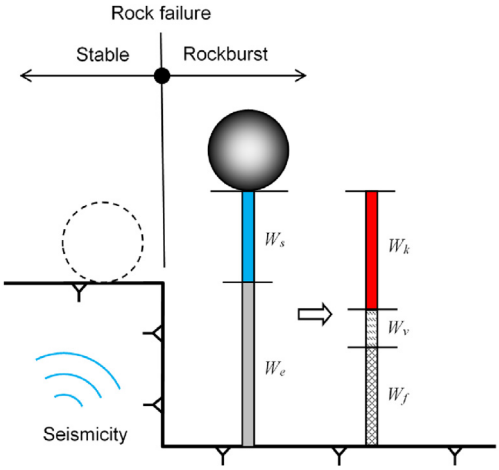

Fig. 11. Conceptual model for rockburst without rock support. W_e is the total released elastic strain energy, W_s is the seismic energy transferred to the ejected rock, W_f is the energy dissipated by rock fracture, W_k is the kinetic energy for rock ejection, and W_v is the energy for vibration and heat. $W_e + W_s = W_f + W_k + W_v$. Note that the energy columns are not to scale.

absorbing yield rockbolts. That support system sustained several small-scale fault-slip rockbursts, even though the rock behind the mesh was finely fragmented. The fine fragmentation of the rock might be due to the satisfactory containment of the support system. The strong surface containment and the reliable link with the rockbolts forced the rock to fragment to dissipate the seismic energy.

In rockburst control, it is required that the support system must be able to provide high resistance in order to restrain rock displacement on the one hand, and it must be deformable on the other hand to dissipate a certain amount of deformation energy. Therefore, all support devices in a support system must be deformable and the reinforcement tendons like rockbolts in the system must be strong. Fig. 16 illustrates a solution for the rock support for rockburst control. The support system comprises obligatory surface-retaining devices (e.g. meshes, straps, shotcrete, and even steel sets), energy-absorbing yield rockbolts, and optional deformable cablebolts. Cablebolts are adopted in extreme cases. The rockbolts must be systematically installed and reliably linked with the surface-retaining devices in the burst-prone areas. With such an integrated support system, the excessive burst energy could be dissipated by the internal reinforcement tendons and the external surface-retaining devices. The portions of the dissipated energy in the reinforcement tendons and the surface-retaining devices are illustrated through the full-scale impact tests introduced below.

Full-scale impact tests of a support system comprised of energy-absorbing yield rockbolts and chain link mesh were carried out to investigate the proportions of energy dissipated in the rockbolts and the mesh (Roth, 2014). The test samples comprised a square concrete slab, rock boulders and gravel on the slab, a sheet of chain link mesh underneath the slab, and four D-bolts, as shown in Fig. 17. The four D-bolts were spaced in a 1.2 m × 1.2 m pattern and were grouted in steel tubes suspended on the frame of the test setup. An impact platform was placed on the rock blocks and gravel. The drop mass hit the platform depending on which impact load was transferred to the test sample. A drop mass of 6280 kg fell from a height of 3.25 m, corresponding to a nominal impact energy of 200 kJ. Two samples were tested. The stiff sample was constructed with a thick concrete slab and large rock blocks to simulate a relatively competent rock mass, while the soft sample had a thin concrete slab and rock fragments to simulate a weak and soft rock mass. Upon impact, the concrete slabs fractured and the bolts and mesh were displaced. The slab and the mesh of the soft sample

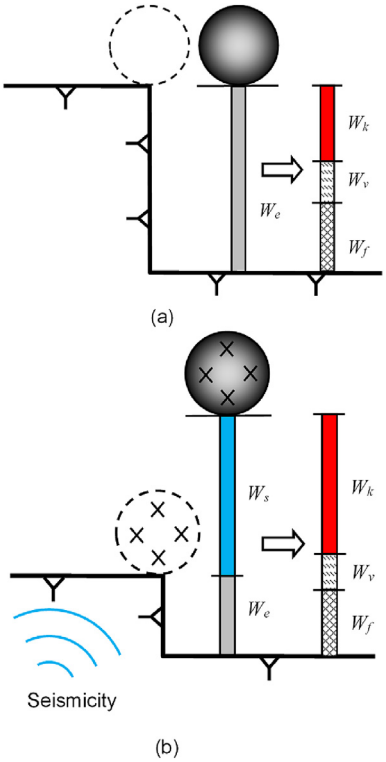

Fig. 12. Conceptual models for (a) self-initiated strain burst and (b) fault-slip rockburst. The crosses in the ball mean that the rock is pre-fractured prior to the burst event.

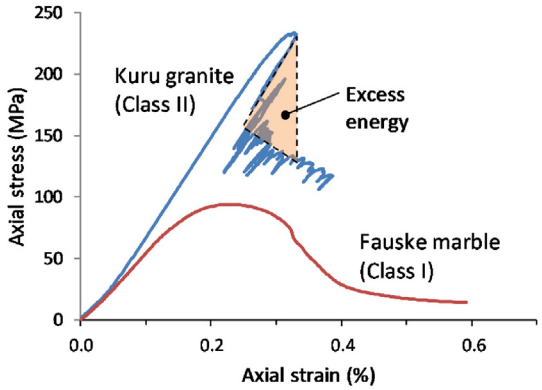

Fig. 13. Stress–strain curves of Class I and Class II rocks.

fractured more and were more deformed than those of the stiff sample. In the stiff sample, the bolts dissipated 32 kJ energy (~75% of the total energy dissipated by the support devices), and the mesh dissipated 8 kJ (~25%). In the soft sample, the bolts dissipated 10 kJ (~30%), and the mesh dissipated 26 kJ (~70%). The rest of the impact energy was dissipated by fragmenting and deforming the rock blocks as well as the energy loss out of the testing system by vibration, etc. The test results implied that rockbolts dissipate more energy than meshes in competent rock mass, while meshes play a more important role than bolts in soft rock mass.

4.2. Requirements

In the case of rockburst, there does not exist a constant load to equilibrate since the support load and the ejection displacement are associated with each other. The support devices in the system must be strong on one hand in order to provide high resistance to the deformation, and on the other hand, they must have high enough energy absorption capacity to prevent premature failure of the support system under the dynamic impact of rockburst. The support devices must also be compatible in deformability.

4.2.1. Energy absorption capacity

Different types of support devices were tried on site in the practice of rockburst control in the past decades. People finally realized that energy-absorbing devices were the most appropriate ones. The load–displacement behavior of three types of support devices is illustrated in Fig. 18. Ductile devices can displace significantly, but their load-bearing capacity is low. Strong and stiff devices can carry high loads but displace little prior to failure. Energy-absorbing devices can both carry high loads and displace significantly. In other words, they can dissipate a significant amount of energy. An energy-absorbing support device is essentially a combination of ductile and strong devices.

4.2.2. Factor of safety

Let W_{rs} represent the energy absorption capacity of the support system for rockburst control. The factor of safety of the support system is expressed as

$$FS = \frac{W_{rs}}{W_k} \tag{2}$$

$$W_k = \frac{1}{2}mv^2 \tag{3}$$

where m is the mass of the ejected rock, and v is the ejection velocity. The ejection velocity can be back calculated based on the horizontally dislodged distance of the ejected rock after a rockburst (Kaiser et al., 1996). Let u_{eq} represent the displacement of the rock after ejection (Fig. 19). This displacement must be smaller than the maximum allowable displacement, u_{max}, which is often decided from the point of view of the excavation operation. On the other hand, u_{eq} must be smaller than the ultimate displacement of the reinforcement tendons (i.e. rockbolts/cables), u_{ult}. The safety criteria for the support system for rockburst control are:

$$FS = \frac{W_{rs}}{W_k} > 1,\ u_{eq} < u_{ult},\ \text{and}\ u_{eq} < u_{max} \tag{4}$$

As seen in the full-scale tests introduced in the previous section, a smaller proportion of energy is dissipated by the surface-retaining mesh than that by the bolts in competent rock mass. Neglecting the energy absorption of the surface-retaining devices, the spacing of the bolts in a systematic bolting support system is calculated from Eq. (2) as

$$s^2 = \frac{1}{FS}\frac{2W_{rs}}{t\rho v^2} \tag{5}$$

where t is the burst depth, and ρ is the density of the rock mass. The bolt length should be at least 1 m longer than the burst depth t (see Fig. 19).

4.2.3. Compatibility between support devices

The current method to support rock in civil tunnels is to install fully encapsulated stiff bolts in the rock mass and to apply shotcrete or cast-in concrete lining on the rock surface. Yield support devices are embedded in the lining in squeezing rock conditions (Schubert, 2001). Rock support systems in civil tunnels are in principle composed of stiff internal reinforcement tendons (fully encapsulated rebar bolts) and flexible external surface-retaining devices (deformation-compensated concrete lining). In such a support system, the stiff internal reinforcement tendons (rockbolts) may fail after a small deformation, but the flexible external support devices (the concrete lining) can accommodate relatively large rock deformation because of the yield devices embedded in the concrete lining. The internal and external devices in the support system are thus not compatible in deformability. In underground mining, yield rockbolts and meshes are often used to deal with excessive rock deformation. The support load is mainly carried by the rockbolts, and the mesh restrains the dilation of the rock on the surface. In such a support system, it seems that the internal reinforcement tendons (the rockbolts) and the external support device (the mesh) are compatible in deformability, but the load-bearing capacity of mesh is very low in the current mine support systems.

In a satisfactory rock support system, both internal and external support devices should be strong and deformable (Li, 2017b). Particularly, they should be compatible in deformability.

5. Methods of rock support

5.1. Reinforcement tendons

Reinforcement tendons refer to rockbolts and cablebolts that are installed in the rock mass. Rockbolts are classified into three categories based on their anchoring mechanisms: discrete-point anchored rockbolt, fully encapsulated rockbolt, and frictional rockbolt (Li, 2017a, c). A discrete-point anchored rockbolt is anchored at one or more positions along the length of the bolt in

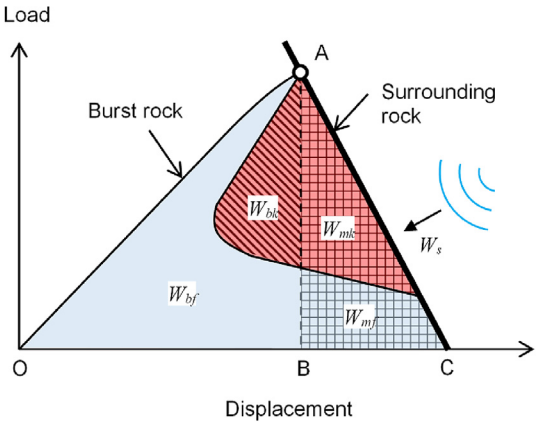

Fig. 14. Conceptual model illustrating the energy components in a rockburst. The strain energy released from the ejected rock is $W_b = W_{bf} + W_{bk}$, the strain energy released from the surrounding rock is $W_m = W_{mf} + W_{mk}$, and W_s is the seismic energy transferred to the ejected rock.

Fig. 15. Rockburst support system comprising strong meshes, mesh straps, and energy-absorbing yield rockbolts in a Canadian deep mine (photo by B. Simser).

the borehole. The mechanical bolt, the cone bolt, the D-bolt, and bulged cablebolts belong to this category. A fully encapsulated rockbolt usually refers to a rebar or threadbar bolt that is grouted with cementitious or resin grout in borehole. The bolt is bonded to the rock mass through the rough surface of the bolt and the grout bond. A frictional rockbolt is anchored in the borehole through the friction between the bolt and the rock. Split Set and inflatable rockbolts, such as Swellex, belong to this category. More details of the three types of rockbolts can be found in Li (2017a, c).

Among the three categories, only the discrete-point anchored bolt has potential for rockburst control because of its relatively high energy-absorbing capacity. The energy-absorbing yield rockbolts currently used for rockburst control are anchored either at two points or at multiple points in the borehole. According to the deformation mechanisms, the discrete-point bolts are classified into stretching and sliding bolts. Stretching bolts accommodate the rock deformation through plastic elongation of the bolt shank. Sliding bolts displace either by plowing of the inner anchor in the grout or by sliding of the bolt shank through the anchor.

5.1.1. Two-point anchored stretching rockbolts

A two-point anchored rockbolt is installed in the borehole either by an expansion shell or by resin grout in the distal end of the bolt. The expansion shell bolt is mechanically anchored in the borehole, and its anchoring capacity is directly proportional to the contact stress between the shell and the rock. An end-grouted rockbolt functions in the same way as an expansion shell bolt in restraining rock deformation. The anchorage of an end-grouted rockbolt is more reliable than an expansion shell bolt because of its strong resin bond. Two-point anchored rockbolts can accommodate a certain amount of rock dilation through the deformation of the bolt plate and the stretch of the bolt shank. It has been used for rockburst control in some hard rock tunnels, such as in Norway.

The distributions of axial and shear stresses along a two-point anchored rockbolt are illustrated in Fig. 20. The rock dilation stretches the bolt shank identically in every cross-section of the shank, resulting in constant axial stress along the length of the bolt. The shear stress on the bolt is zero. The ultimate axial stress in the bolt is associated with either the plate strength or the anchoring capacity at the far end of the bolt.

5.1.2. Multi-point anchored stretching rockbolts

The D-bolt is an energy-absorbing yield rockbolt with several anchors along the bolt length and smooth bar sections between the anchors, as shown in Fig. 21a. The bolt is fully encapsulated in the borehole, either with cementitious grout or resin. The anchors are fixed in the grout, and the smooth bar sections elongate upon rock dilation. The bolt dissipates a quite large amount of energy by fully employing the strength and deformation capacity of the bolt's steel (Li and Doucet, 2012).

The distributions of axial and shear stresses along a D-bolt are illustrated in Fig. 21b. The stresses in a section between two adjacent anchors are induced by the total dilation of the rock that the smooth bar section traverses. The ultimate load of the D-bolt is equal to the ultimate tensile load of the bolt shank.

5.1.3. Cablebolts

Cablebolts are made of a single strand, twin strands, or multiple strands. They usually are encapsulated with cementitious grout in boreholes. The cable wires are made by cold extrusion, and their ultimate elongation is low, only 3%–5%. To enhance the deformation capacity of cablebolts, a widely used technique is to de-bond the middle section of the cable from the cementitious grout with a plastic sleeve. For example, the ultimate displacement of a 10-m cable is increased by 0.2 m if the cable is de-bonded for 5 m in the middle with an assumption that the ultimate strain of the cable wires is 4%.

5.1.4. Sliding rockbolts

The cone bolt is a representative one among the several sliding energy-absorbing yield rockbolts available at present (Fig. 22a). The

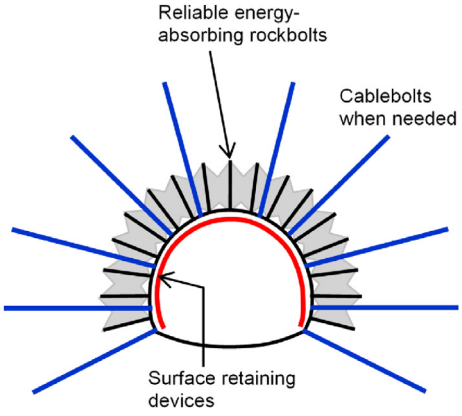

Fig. 16. Schematic illustration of a support system for rockburst control.

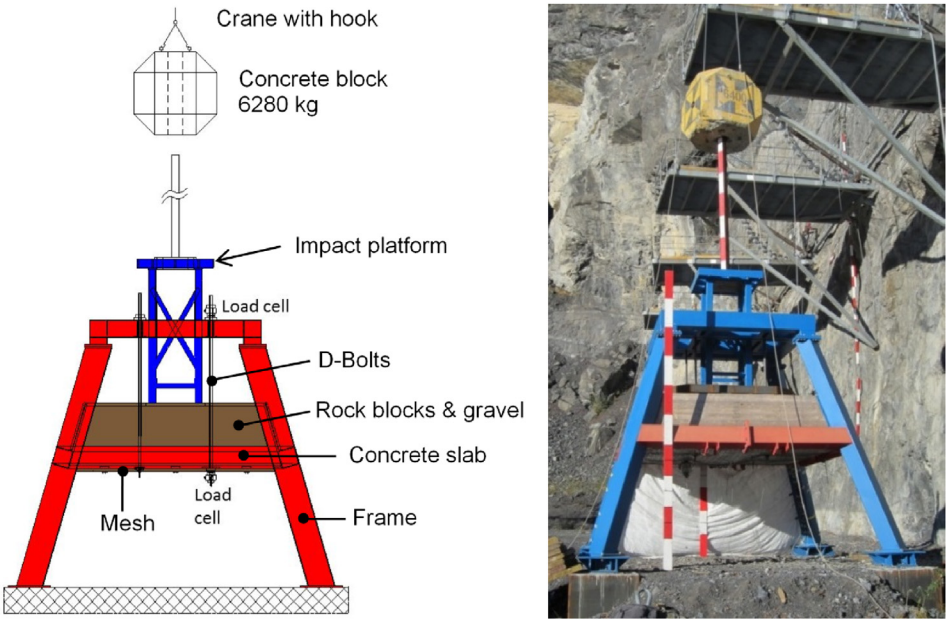

Fig. 17. The setup for the full-scale impact tests (Roth, 2014).

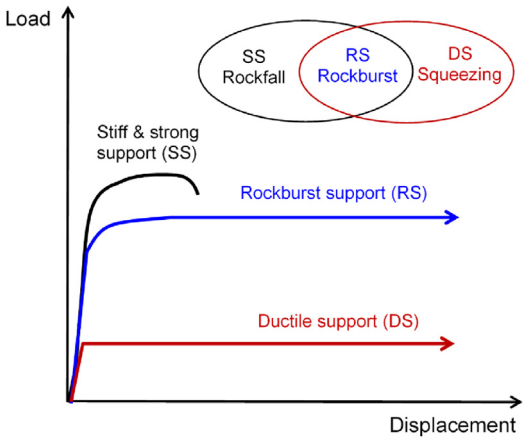

Fig. 18. Sketch of the load–displacement behavior of ductile, strong, and energy-absorbing support devices.

cone bolt is a smooth steel bar with conical flaring at the distal end. The original version of the bolt is for cementitious grout and the modified version is for resin grout. The cone bolt is fully grouted in the borehole. Rock dilation results in a load on the bolt plate that transfers the pull load to the cone at the distal end via the bolt shank that is de-bonded from the grout due to the smoothness of the cylindrical surface of the bolt. The cone plows in the grout when the load is equal to the crushing strength of the grout. The distributions of axial and shear stresses along a cone bolt, as sketched in Fig. 22b, are similar to that of two-point anchored conventional bolts, but the ultimate load of the cone bolt is determined by the plowing load of the cone at the distal end.

5.2. Surface retaining devices

5.2.1. Mesh

Mesh is often used for surface containment in mines. The two most frequently used types are welded mesh and chain-link mesh (Fig. 23). Welded mesh is manufactured by welding at the intersections of the grids, while chain-link mesh is made by weaved wires. Meshes are laid on exposed rock surfaces and linked to rockbolts by the bolt plates. The grid size of the welded mesh is usually 75 mm or 100 mm. Welded mesh is stiffer than chain-link mesh, and the deflection capacity of chain-link mesh is greater than that of welded mesh.

5.2.2. Mesh strap

Mesh strap is laid over meshes or mesh-shotcrete to enhance the surface retaining capacity of the surface-retaining liner (Fig. 24). A mesh strap is approximately 0.3 m wide and made of 8-mm steel bars. Strap meshes are widely used in Canadian and Australian metal mines.

5.2.3. Lacing

The purpose of lacing is also to enhance the surface-retaining capacity of the meshes. Cables of 11 mm in diameter are laid over meshes in a certain pattern and are nailed into the rock with 0.6-m long eyebolts at the intersections of the cables (Fig. 25). The lacing-mesh system can accommodate a large amount of surface dilation and provide satisfactory containment to fragmented rock.

5.2.4. Shotcrete

Shotcrete has been widely used for rock support in civil and mining engineering for a long time. Fiber-reinforced shotcrete is more used than plain shotcrete because the former significantly improves the toughness of the concrete. The dotted line in Fig. 26 shows the load on a steel fiber-reinforced shotcrete (SFRS) panel versus its deflection. The slab did not lose its load-bearing capacity immediately after the peak load. Instead, it continued to carry a certain load in the post-peak stage.

Mesh-reinforced shotcrete is also used in rock support practices. Mesh is either embedded in or laid over the shotcrete layer. The load-bearing capacity of mesh-embedded shotcrete is slightly higher than that of mesh-overlaid shotcrete, but the mesh-overlaid shotcrete can accommodate larger displacements. The load–displacement curves of the two types of mesh-reinforced shotcrete panels are presented in Fig. 26. Mesh embedded in the shotcrete could rupture after a small fracture opening in the

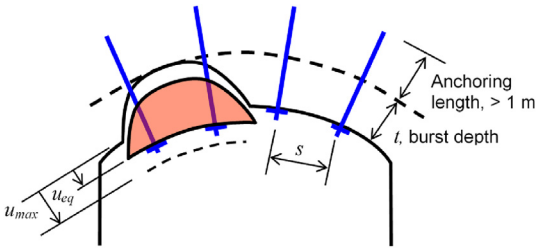

Fig. 19. Displacements, u_{eq} and u_{max}, in a rockburst and bolting pattern (Li, 2017a).

shotcrete (Fig. 27a), while mesh laid on the top of the shotcrete can sustain the fractured shotcrete for a large displacement before its support function is lost (Fig. 27b).

5.3. Examples of rockburst support systems

The rockbolts in a support system reinforce the surrounding rock, while the surface-retaining devices, such as mesh, prevent small rock pieces from falling. The surface-retaining devices must be linked firmly with the rockbolts to achieve an optimum reinforcement effect. In reality, the link between the mesh and the bolts is often weak (Simser, 2007). With weak links, the load on the mesh cannot be transferred to the rockbolts. Fig. 28a shows a situation in which the mesh was cut off and lost the link with the rockbolts. Fig. 28b shows a support system in a deep mine that had satisfactory links between the rockbolts and the meshes and mesh straps.

5.3.1. Soft support system

The support systems used for rockburst control in Australian mines, such as the one in Longshaft mine (Li, 2008), at the beginning of the 21st century typically comprised two passes (Fig. 29). Pass 1 comprised 2.4-m long Split Set bolts in a 1.2 m × 1.2 m bolting pattern and meshes on rock surface, which aimed to static support. In Pass 2, extra devices, such as SFRS over the mesh and 6-m long fully grouted plain cables, were installed for rockburst control. Some mines, such as Argot and Junction mines, used yield cables instead of fully grouted plain cables to improve the ductility of the support system.

Both Split Set bolts and cables in the support system are yieldable. The Split Set bolts yield at quite low load levels. Therefore, such a system is called a soft support system. The major advantage of such a soft support system is its large deformation capacity, but it cannot dissipate much energy. Soft support systems cannot satisfactorily control strong rockburst. In recent years, some Australian mines have started to replace Split Sets with stronger energy-absorbing yield rockbolts in their support systems for rockburst control.

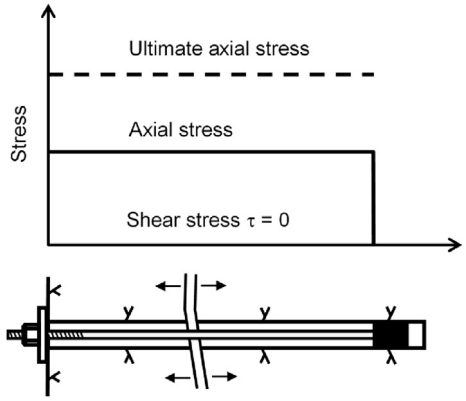

Fig. 20. Model for the axial and shear stresses along a conventional two-point anchored rockbolt.

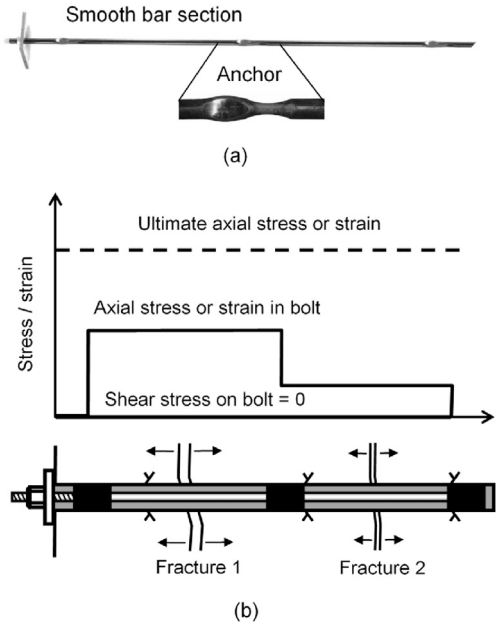

Fig. 21. (a) The D-bolt, and (b) a model for the distributions of axial and shear stresses along the D-bolt.

5.3.2. Stiff and yieldable hybrid support system

In Canadian metal mines, the rockbolts usually used for static support are 2.4 m or 2.1 m long fully encapsulated rebar bolts and Split Set bolts. Energy-absorbing yield rockbolts are added for rockburst control. Meshes and mesh straps are widely used.

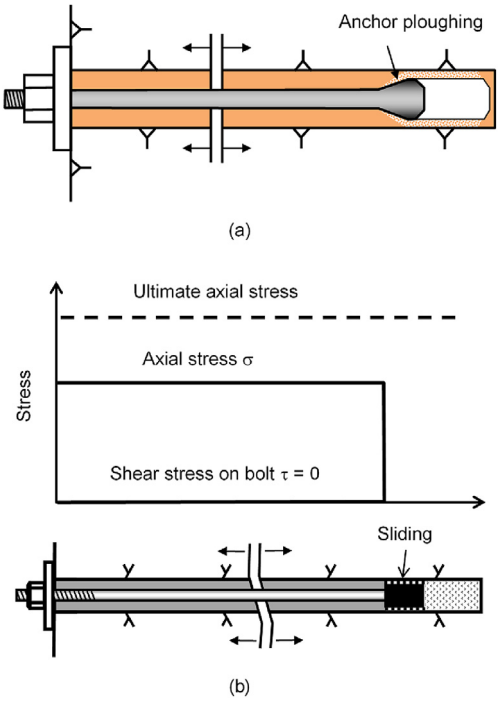

Fig. 22. The cone bolt: (a) A sketch illustrating the work principle and (b) a model for the distributions of axial and shear stresses along a cone bolt.

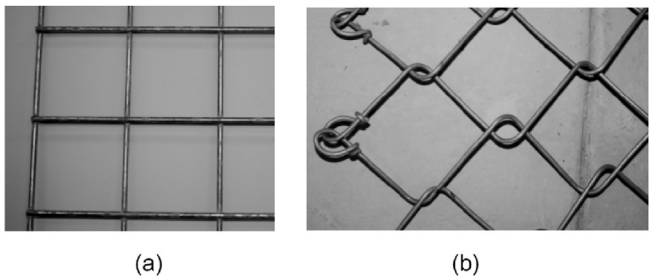

Fig. 23. Two types of meshes: (a) Welded mesh and (b) chain-link mesh (Player et al., 2008).

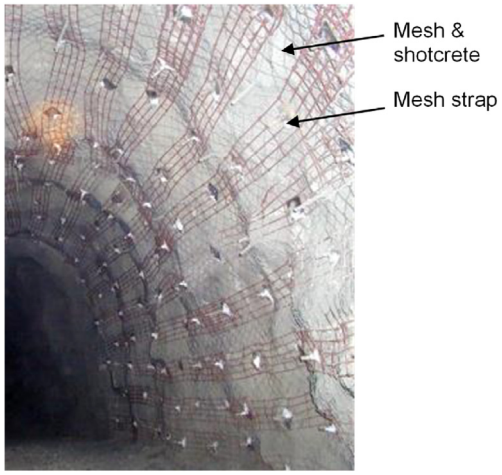

Fig. 24. Mesh-shotcrete overlaid by mesh straps (Louchnikov et al., 2014).

Shotcrete sometimes is used. A support system for rockburst control typically is installed in two passes, and sometimes in three. Pass 1 is for static support, and Passes 2 and 3 are for rockburst control. The support devices installed in Pass 1 are typically fully encapsulated rebar bolts and mesh, such as those in the Craig mine, but Split Set bolts are used in some other mines, such as the Creighton mine. The support devices installed in Pass 2 are mesh straps and energy-absorbing yield bolts, and they are de-bonded cables in Pass 3.

Various support systems for rockburst control were used in the Craig mine in the early 2000s, which are illustrated in Fig. 30 (Li, 2008). In Pass 1, fully encapsulated rebar bolts were installed in the roof and walls, and meshes were laid over the rock surfaces. In Pass 2, mesh straps, either in the lateral orientation or in both

Fig. 25. Lacing on the wall of a deep mine drift in South Africa.

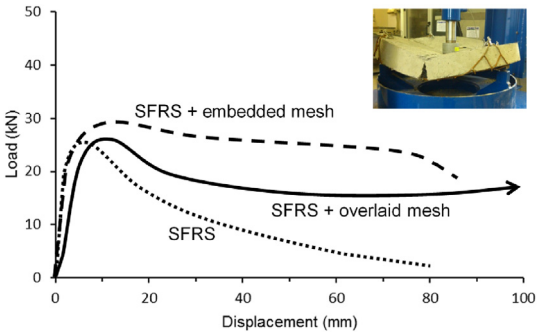

Fig. 26. Deflection tests of 75-mm thick SFRS panels without and with mesh reinforcements. Redrawn after Swedberg et al. (2014).

lateral and longitudinal orientations, were laid over the meshes and nailed into the ground with modified cone bolts (MCBs) (Fig. 30a and b). When needed (Pass 3), fully grouted de-bonded cables were installed in the roof (Fig. 30c). Sometimes two cable strands were installed in one borehole, with one strand being fully grouted and the other one being de-bonded.

Fig. 31 illustrates the support system for rockburst control quite widely used in Canadian metal mines. In the system, two-point anchored yield bolts, typically resin-grouted MCBs, are placed between stiff rebar bolts. The philosophy for such an arrangement is that the stiff rebar bolts restrain the bulking of the rock under the static loading condition, and the cone bolts undertake the dynamic loads when rockburst occurs. Static rock support requires the bolt quick response to rock deformation so that the bolts provide support load as long as rock deformation occurs in the rock mass. In other words, it requires rockbolts to be of high stiffness. Use of fully


(a)

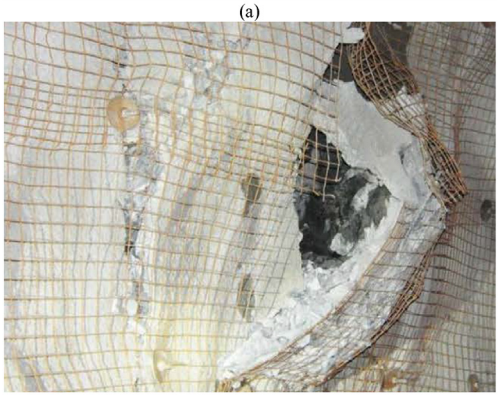
(b)

Fig. 27. (a) Broken mesh wires in embedded shotcrete in situ (photo by B. Simser) and (b) the behavior of overlaid mesh shotcrete (Malmgren et al., 2014).

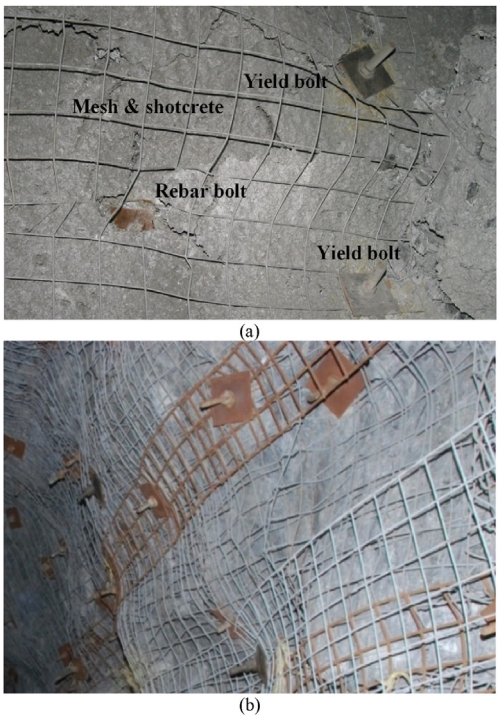

Fig. 28. Link between rockbolts and the surface-retaining meshes and mesh straps: (a) Weak links and (b) satisfactory links.

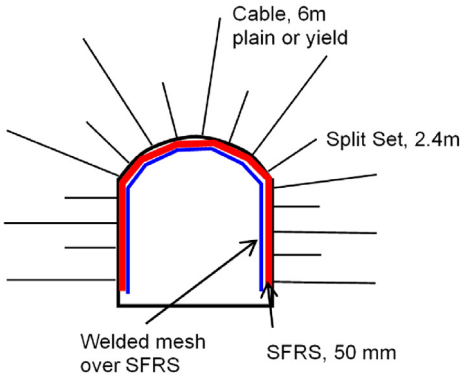

Fig. 29. A soft ground support system used in Longshaft gold mine (Li, 2008).

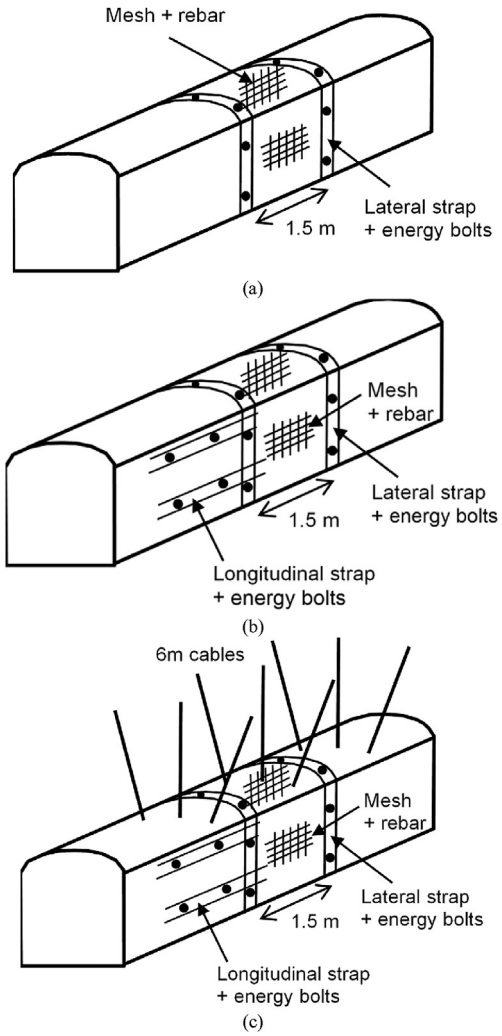

Fig. 30. Support systems for rockburst control used in the Craig mine, Canada: (a) The single-strap system, (b) the double-strap system, and (c) the strap-and-cable system (Li, 2008).

encapsulated bolts is proper for this purpose. However, stiff rebar bolts would easily rupture when rockburst occurs, as the case shown in Fig. 1a. The cone bolt can accommodate significant displacements so that it could be used for rockburst control. The major drawback of the cone bolt as a static support device is that its elastic stiffness is much lower than that of the rebar bolt. This implies that the cone bolt is not able to provide high enough support load until a relatively large amount of rock displacement has occurred. In addition, the load-bearing capacity of MCBs is much dependent on the mixing quality of the resin capsules that is always an issue on site. Furthermore, the anchoring reliability of the cone bolt is a concern because of its two-point anchoring mechanism. Failure of any one of the two anchors will lead to loss of the reinforcement function of the bolt. Because of those concerns, on-site engineers do not dare to only use cone bolts in rock support systems for rockburst control. In the early 2000s, the cone bolt was the sole yield bolt that could be used for rockburst control. Ground control engineers started to mix rebar bolts and cone bolts in their support systems for rockburst control. Therefore, the hybrid support system illustrated in Fig. 31 was a compromise solution when only rebar and cone bolts, or other types of two-point anchored yield rockbolts, were available at that time even though it is still used today. The ideal support system should comprise only one type of rockbolt that is able to provide reinforcement functions under both static and dynamic loading conditions. Such a type of rockbolt must be elastically stiff but plastically deformable when the load is beyond a certain level.

5.3.3. *Entirely yieldable support system*

Serious rockbursts started to appear in the Kiruna iron ore mine in Sweden in the late 1990s. The early support system for rockburst control in the mine was developed from the static support system at that time. It comprised 4 passes: Pass 1 was installation of fully cement-grouted rebar bolts and SFRS; Pass 2 was installation of Swellex; Pass 3 was 7-m long cable; and Pass 4 was to construct shotcrete arches (Li, 2008). The system did not perform well, possibly due to its high stiffness. After recognizing the importance of deformability and energy absorption capacity of support devices, the mine developed a system consisting entirely of yield devices.

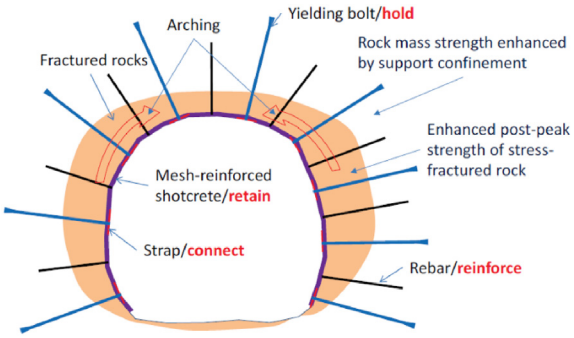

Fig. 31. Rockburst support system using integrated stiff and yield rockbolts (Cai and Kaiser, 2018).

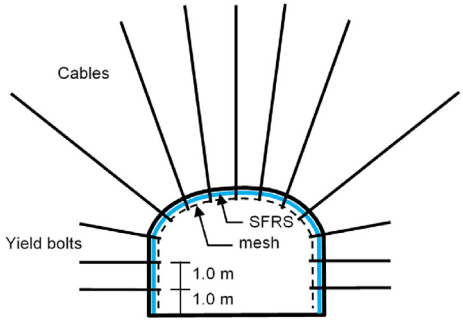

Fig. 32. The current rockburst support system of the Kiruna iron ore mine in Sweden (Malmgren et al., 2014).

That system comprises a 100-mm thick SFRS layer, wire mesh over the SFRS layer, 3-m long modified and deformable rebar bolts or D-bolts in a 1 m × 1 m bolting pattern in the walls, and 7-m long cablebolts in the roof (Fig. 32). This support system has sustained several large rockbursts without uncontrollable consequences in the past several years.

6. Conclusions

In highly stressed hard and massive rock mass, surface-parallel extension fractures often occur in the ejected and surrounding rocks when a strain burst occurs. In highly stressed, moderately hard rock mass, a fracture zone is created in the surrounding rock during tunnel excavation. Fault-slip rockburst could occur in the fracture zone.

Excessive release energy is prerequisite for the occurrence of rockburst. The excessive energy comes from the ejected rock itself and the surrounding rock. The energy absorption capacity (W_{rs}) of a support system for rockburst control must be larger than the excessive energy.

All support devices in a support system should be able to dissipate energy, be firmly linked, and be compatible in deformability. A support system for rockburst control comprises in general three support layers, that is, a layer of fully surface-covered retaining devices (mesh, mesh strap and shotcrete), a layer of systematic yield rockbolts and a layer of yield cablebolts (optional). Overlaying mesh on fiber-reinforced shotcrete is a good way to enhance the surface-retaining capacity of the support system. The internal reinforcement tendons (rockbolts and cablebolts) dissipate more energy than surface-retaining devices (mesh and shotcrete) in competent rock mass, while more energy is dissipated in surface-retaining devices in soft and weak rock mass.

Several types of energy-absorbing yield rockbolts are available for rockburst control. Those bolts dissipate energy either by stretching of the bolt shank or sliding of the inner anchor in the borehole. Available surface-retaining devices are mesh, mesh strap, and fiber-reinforced shotcrete.

Soft support system is not competent for rockburst control. Hybrid stiff and yield support system is not satisfactory because of the difference in deformability of the stiff and yield rockbolts. Entirely yieldable support system seems to be the best option for rockburst control.

Declaration of competing interest

The author declares that he has no known competing financial interests or personal relationships that could have appeared to influence the work reported in this paper.

References

Andersson, J.C., Martin, C.D., Stille, H., 2009. The Äspö pillar stability experiment: Part II — rock mass response to coupled excavation-induced and thermal-induced stresses. Int. J. Rock Mech. Min. Sci. 46 (5), 879–895.
Cai, M., Kaiser, P.K., 2018. Rock Support Reference Book. In: Rockburst Phenomenon and Support Characteristics, vol. 1. MIRARCO Mining Innovation, Sudbury, Canada.
Cook, N.G.W., Ortlepp, W.D., 1968. A yielding rock bolt. Chamber of Mines of South Africa Research Organisation Bulletin, No. 14, pp. 6–8.
Darlington, B., Rataj, M., Balog, G., Barnett, D., 2018. Development of the MDX bolt and in-situ dynamic testing at Telfer gold mine. In: Li, C.C., Li, X., Zhang, Z.X. (Eds.), Rock Dynamics and Applications 3: Proceedings of the 3rd International Conference on Rock Dynamics and Applications (RocDyn-3). CRC Press, pp. 403–408.
Diederichs, M.S., 2003. Manuel Rocha Medal Recipient Rock fracture and collapse under low confinement conditions. Rock Mech. Rock Eng. 36 (5), 339–381.
Duvall, W.I., Stephenson, D.E., 1965. Seismic energy available from rock bursts and underground explosions. Society of Mining Engineers, pp. 235–240.
Feng, X.T., Chen, B.R., Ming, H.J., Wu, S.Y., Xiao, Y.X., Feng, G.G., Zhou, H., Qiu, S.L., 2012. Evolution law and mechanism of rockbursts in deep tunnels: immediate rockburst. Chin. J. Rock Mech. Eng. 31 (3), 433–444 (in Chinese).
Feng, X.T., Xiao, Y.X., Feng, G., Chen, B.R., Li, S., 2018. Successful examples for mitigating rockbursts in Jinping II tunnels, China. In: Feng, X.T. (Ed.), Rockburst: Mechanisms, Monitoring, Warning and Mitigation. Elsevier, pp. 519–539.
He, M., Gong, W., Wang, J., Qi, P., Tao, Z., Du, S., Peng, Y., 2014. Development of a novel energy-absorbing bolt with extraordinarily large elongation and constant resistance. Int. J. Rock Mech. Min. Sci. 67, 29–42.
He, M.C., Miao, J.L., Feng, J.L., 2010. Rockburst process of limestone and its acoustic emission characteristics under true-triaxial unloading conditions. Int. J. Rock Mech. Min. Sci. 47 (2), 286–298.
Jager, A.J., 1992. Two new support units for the control of rockburst damage. In: Kaiser, P.K., McCreath, D.R. (Eds.), Rock Support in Mining and Underground Construction: Proceedings of the International Symposium on Rock Support. A.A. Balkema, Rotterdam, Netherlands, pp. 621–631.
Kaiser, P.K., Tannant, D.D., McCreath, D.R., 1996. Canadian Rock Burst Support Handbook. Geomechnaics Research Center at MIRARCO Mining Innovation, Sudbury, Canada.
Kaiser, P.K., 2018. Excavation vulnerability and selection of effective rock support to mitigate rockburst damage. In: Feng, X.T. (Ed.), Rockburst: Mechanisms, Monitoring, Warning and Mitigation. Elsevier, pp. 473–518.
Knox, G., Berghorst, A., 2019. Dynamic testing: determining the residual dynamic capacity of an axially strained tendon. In: Hadjigeorgiou, J., Hudyma, M. (Eds.), Ground Support 2019: Proceedings of the 9th International Symposium on Ground Support in Mining and Underground Construction. Australian Center for Geomechanics, Perth, Australia, pp. 231–242.
Li, C., Nordlund, E., 1993. Experimental verification of the Kaiser effect in rocks. Rock Mech. Rock Eng. 26 (4), 333–351.
Li, C.C., Doucet, C., 2012. Performance of D-bolts under dynamic loading conditions. Rock Mech. Rock Eng. 45 (2), 193–204.
Li, C.C., 2010. A new energy-absorbing bolt for rock support in high stress rock masses. Int. J. Rock Mech. Min. Sci. 47 (3), 396–404.
Li, C.C., 2017c. Energy-absorbing rockbolts. In: Feng, X.T. (Ed.), Rock Mechanics and Engineering. Excavation, Support and Monitoring, vol. 4. CRC Press, Boca Raton, USA, pp. 311–336.
Li, C.C., 2017b. Principles of rock bolting design. J. Rock Mech. Geotech. Eng. 9 (3), 396–414.
Li, C.C., 2017a. Rockbolting: Principles and Applications. Butterworth-Heinemann.
Li, C.C., 2019. Rockburst conditions and rockburst support. Chin. J. Rock Mech. Eng. 38 (4), 674–682 (in Chinese).
Li, C.C., 2008. State of the art on ductile ground support systems and elements. Commission Report. Rock Tech. Center, Luleå, Sweden.

Li, D., Sun, Z., Xie, T., Li, X., Ranjith, P.G., 2017. Energy evolution characteristics of hard rock during triaxial failure with different loading and unloading paths. Eng. Geol. 28, 270–281.
Louchnikov, V., Sandy, M.P., Watson, O., Orunesu, M., Eremenko, V., 2014. An overview of surface rock support for deformable ground conditions. In: 12th AusIMM Underground Operators' Conference. Adelaide, Australia.
Malmgren, L., Swedberg, E., Krekula, H., Woldemedhin, B., 2014. Ground support at LKAB's underground mines subjected to dynamic loads. In: Workshop on Ground Support Subjected to Dynamic Loading. Sudbury, Canada.
Martin, C.D., Chandler, N.A., 1994. The progressive fracture of Lac du Bonnet granite. Int. J. Rock Mech. Min. Sci. Geomech. Abstr. 31 (6), 643–659.
Morrison, D., Swan, G., Kaiser, P., McCreath, D., Tannant, D., Neumann, M., Kazakadis, V., Talebi, S., 1996. Canadian Rockburst Research Program 1990–1995: A Comprehensive Summary of Five Years of Collaborative Research on Rockbursting in Hardrock Mines. Canada CAMIRO Mining Division.
Morrison, R.G.K., 1942. Report on rockburst situation in Ontario mines. Trans. Can. Inst. Min. Metall. Min. Soc. N. S. 45, 225–272.
Ortlepp, W.D., 1969. An empirical determination of the effectiveness of rock bolt support under impulse loading. In: Brekke, T.L., Jorstad, F.A. (Eds.), Proceedings of the International Symposium on Large Permanent Underground Openings. Australian Center for Geomechanics, Oslo, Australia, pp. 197–205.
Ortlepp, W.D., 1997. Rock Fracture and Rockbursts – An Illustrative Study. South African Institute of Mining and Metallurgy, Johannesburg, South Africa.
Ortlepp, W.D., 1992. The design of support for the containment of rockburst damage in tunnels – an engineering approach. In: Kaiser, P.K., McCreath, D.R. (Eds.), Rock Support in Mining and Underground Construction. A.A. Balkema, Rotterdam, Netherlands, pp. 593–609.
Player, J.R., Morton, E.C., Thompson, A.G., Villaescusa, E., 2008. Static and dynamic testing of steel wire mesh for mining applications of rock surface support. In: 6th International Symposium on Ground Support in Mining and Civil Engineering Construction. Cape Town, South Africa, pp. 693–706.
Roth, A., 2014. Full scale tests of mesh in combination with rockbolts subjected to dynamic loading. In: Workshop on Ground Support Subjected to Dynamic Loading. Sudbury, Canada.
Salamon, M.D.G., 1983. Rock burst hazard and the fight for its alleviation in South African gold mines. In: Proceedings of Rockbursts Prediction and Control. Institute of Mines and Metallurgy, London, UK, pp. 11–36.
Schubert, W., 2001. Recent experience with squeezing rock in Alpine tunnels. In: Allan, C. (Ed.), Proceedings of CUC – Rock Support in Medium to Poor Rock Conditions. Sargans, Switzerland.
Shan, Z.G., Yan, P., 2010. Management of rock bursts during excavation of the deep tunnels in Jinping II Hydropower station. Bull. Eng. Geol. Environ. 69 (3), 353–363.
Simser, B., Andrieux, P., Mercier-Langevin, F., Parrott, T., Turcotte, P., 2006. Field behaviour and failure modes of modified conebolts at the Craig, LaRonde and Brunswick mines in Canada. In: Challenges in Deep and High Stress Mining. Australia Center for Geomechancis, Perth, Australia.
Simser, B., 2001. Geotechnical Review of the July 29th, 2001 West Ore Zone Mass Blast and the Performance of the Brunswick/NTC Rockburst Support System. Technical Report.
Simser, B., 2007. The weakest link – ground support observations at some Canadian shield hard rock mines. In: Potvin, Y. (Ed.), Proceedings of the 4th International Seminar on Deep and High Stress Mining. Australian Center for Geomechanics, Perth, Australia, pp. 335–348.
Stacey, T.R., 2012. A philosophical view on the testing of rock support for rockburst conditions. J. S. Afr. Inst. Min. Metall 112, 703–710.
Su, G.S., Feng, X.T., Wang, J.H., Jiang, J.Q., Hu, L.H., 2017. Experimental study of remotely triggered rockburst induced by a tunnel axial dynamic disturbance under true-triaxial conditions. Rock Mech. Rock Eng. 50 (9), 2207–2226.
Swedberg, E., Thyni, F., Töyrä, J., Eitzenberger, A., 2014. Rock support testing in Luossavaara-Kirunavaara AB's underground mines, Sweden. In: Hudyma, M., Potvin, Y. (Eds.), Deep Mining 2014: Proceedings of the 7th International Conference on Deep and High Stress Mining. Australian Center for Geomechanics, Sudbury, Canada, pp. 139–150.
Tarasov, B.G., Stacey, T.R., 2017. Features of the energy balance and fragmentation mechanisms at spontaneous ailure of Class I and Class II rocks. Rock Mech. Rock Eng. 50 (10), 2563–2584.
Varden, R., Lachenicht, R., Player, J., Thompson, A., Villaescusa, E., 2008. Development and implementation of the Garford dynamic bolt at the Kanowna Belle mine. In: 10th Underground Operators' Conference. The Australian Institute of Mining and Metallurgy, Launceston, Australia, pp. 95–104.
Wawersik, W.R., Fairhurst, C., 1970. A study of brittle rock fracture in laboratory compression experiments. Int. J. Rock Mech. Min. Sci. Geomech. Abstr. 7 (5), 561–575.
Wu, Y.K., Oldsen, J., 2010. Development of a new yielding rock bolt – yield-Lok bolt. In: Proceedings of the 44th US Rock Mechanics Symposium and 5th US-Canada Rock Mechanics Symposium. Curran Associates, Inc., pp. 1378–1383

Charlie Chunlin Li is a professor of rock mechanics for civil and mining engineering in the Norwegian University of Science and Technology (NTNU) in Norway. He is in charge of the teaching and research program in rock mechanics in the university. Li obtained his BSc and MSc degrees in Central South Institute of Mining and Metallurgy, China, in 1981 and 1984, respectively, and PhD degree in Lulea University of Technology (LUT), Sweden, in 1993. His work experience includes research associate and associate professor in LUT, ground control engineer in Boliden Mineral Ltd., Sweden, chief technical officer in Dynamic Rock Support AS, Norway, and professor in NTNU. His expertise is in stability analyses of underground space and ground control. In the last two decades, his research interest has been focused on the performance of rockbolts and rock support in difficult rock conditions. He invented the D-bolt that has been worldwide used for rockburst control in deep underground mines. He published a book entitled *Rockbolting – Principles and Applications*. He is a member of the Norwegian Academy of Technological Sciences (NTVA). He was the International Society for Rock Mechanics and Rock Engineering (ISRM) Vice-President for Europe 2015–2019.